Available online at www.sciencedirect.com
SCIENCE DIRECT
Journal of Catalysis 229 (2005) 252–258
JOURNAL OF CATALYSIS
www.elsevier.com/locate/jcat

Selective hydrogenation of 1,3-butadiene on $Pt_3Sn(111)$ alloys: comparison to Pt(111)

Y. Jugnet *, R. Sedrati, J.C. Bertolini

Institut de Recherches sur la Catalyse - CNRS, 2 avenue A. Einstein, F-69626 Villeurbanne cedex, France

Received 30 July 2004; revised 28 September 2004; accepted 30 September 2004

Abstract

The reactivity of $Pt_3Sn(111)$ has been tested in the 1,3-butadiene hydrogenation reaction and compared to that of Pt(111) by a combination of polarization modulation absorption reflection infrared spectroscopy, mass spectroscopy and gas phase chromatography techniques. $Pt_3Sn(111)$ is less active than Pt(111) by one order of magnitude but it is more selective into butenes whatever the initial surface structure $p(2 \times 2)$ or $(\sqrt{3} \times \sqrt{3})$.

Keywords: Surfaces; Butadiene hydrogenation; In situ PM-RAIRS; Pt(111); $Pt_3Sn(111)$

1. Introduction

Selectively hydrogenating 1,3-butadiene to butenes is an efficient route to upgrade the C4 cuts produced in naphta steam crakers and as such this reaction has been widely studied on various transition and noble metals mostly on supported catalysts [1–3]. Actually, palladium is a widely used catalyst for this reaction. Its catalytic performances can be largely improved by the addition of a promoter or a second metal. Furthermore, coke formation is generally significantly reduced in bimetallic catalysts. However, there is still a need for catalysts showing a high selectivity into 1-butene, a by-product used for the production of low density polyethylene.

The catalytic activity and selectivity are driven by numerous factors such as the nature of the catalyst and of its support, the pretreatment of the catalyst, its ability to dissociate hydrogen, the temperature and partial pressure of reactants, the relative adsorption strengths of butadiene and butenes... They are modified by addition of a promoter or the use of an alloy.

A rather detailed knowledge of the parameters at the origin of enhanced catalytic activities and selectivities is highly desirable. Single crystal studies already appeared highly relevant for modelling the behaviour of high surface area supported catalysts since they exclude metal support interactions and in addition, by using standard cleaning procedures, reproducible catalysts can be prepared. Such studies provide valuable information relative to the structure sensitivity [4,5], to the characterization of the adsorption sites and geometries [6,7], to the competitive adsorption of reactants and semihydrogenated by-products [8], and possibly to the identification of intermediate surface species or poisons of the reaction.

From these model studies, it appears that Pd(110) is the best monometallic catalyst showing a catalytic activity of 210^{15} mol cm^{-2} s^{-1}, i.e., a turnover frequency close to 2 s^{-1} and a selectivity into butenes of 100% at 50% conversion [9] at 300 K and a pressure of hydrogen of 10 Torr. As observed for supported catalysts, these properties of Pd can still be largely enhanced by alloying effects [5].

The reactivity of platinum single crystals has been also investigated in this reaction [4,8,10]. It is certainly less performant than palladium, however once alloyed to Ni for example, both its activity and selectivity are improved [11].

* Corresponding author. Fax number: +33 4 72 44 53 99.
E-mail address: jugnet@catalyse.cnrs.fr (Y. Jugnet).

0021-9517/$ – see front matter
doi:10.1016/j.jcat.2004.09.028

Actually, in bulk or surface alloy compounds, the thermodynamic equilibrium induces particular rearrangement of atoms and generates specific local structures available for the reaction [5]. Indeed surface structure and catalytic properties are intimately correlated. In this respect, $Pt_3Sn(111)$ appears as very promising for testing such a reaction since it shows two superstructures with different kinds of Pt atom arrangement in the surface layer. Furthermore, PtSn supported catalysts have been widely investigated for various reactions such as hydrogenation of organic molecules [12–14] and hydrocarbon dehydrogenation [15,16] or reforming [17].

In this study, we present first results of 1,3-butadiene hydrogenation obtained on an alloy of platinum with tin, the $Pt_3Sn(111)$. The surface of this alloy which has been widely studied by Bardi et al. [20], namely by a combination of X-ray photoelectron spectroscopy (XPS), ion scattering spectroscopies, standard and spot profile analysis low energy electron diffraction (LEED and SPA-LEED), and scanning tunnelling microscopy (STM), displays several surface structures depending on the annealing temperature. A $(\sqrt{3} \times \sqrt{3})$ ordered structure is obtained at moderate temperature while a $p(2 \times 2)$ structure is obtained at higher temperature. The corresponding top surface layers show specific Pt atom arrangements which could be at the origin of specific catalytic properties. Both surfaces $(\sqrt{3} \times \sqrt{3})$ and $p(2 \times 2)$ of $Pt_3Sn(111)$ have been investigated and compared to Pt(111) in the 1,3-butadiene hydrogenation reaction under identical conditions. The reaction and by-products formation have been analysed by a combined polarization modulation reflection absorption infrared spectroscopy (PM-RAIRS) operated under elevated pressures, quadrupole mass spectroscopy (QMS) and gas phase chromatography.

2. Experimental

The experimental set-up consists of three main chambers separated by gate valves with various probes to allow the sample to be transferred between all three chambers under ultra high vacuum (UHV). The first two UHV chambers, dedicated to sample preparation and surface characterization, have a base pressure in the low 10^{-10} Torr range. They are equipped with XPS, high resolution electron energy loss spectroscopy (HREELS), and a quadrupole mass spectrometer (QMS). The third chamber is a small stainless steel reactor previously described [21], equipped with two ZnSe infrared windows allowing infrared measurements in a large range of pressure from UHV up to atmospheric pressure. The volume of the reactor is about 1 l. Analysis of products is generally made by mass spectroscopy through a leak valve. A small chamber (a few cm^3) equipped with a septum has been added to the reactor in order to sample the reaction mixture with the help of a syringe (1 ml), allowing injection into a gas phase chromatograph for analysis of the butene isomers.

The PM-RAIR spectra were obtained from a NEXUS Fourier transform infrared spectrometer from Thermo Nicolet within the following configuration. The external IR beam is focused on the sample inside the reactor at a grazing angle (8°) via a parabolic mirror. The incident beam is intercepted by a ZnSe polarizer and a photoelastic modulator (PEM-90 from HINDS instruments) allowing very rapid polarization changes. The polarizer allows the selection of the p-polarized (light polarized in the plane of incidence) or of the s-polarized (light perpendicular to the plane of incidence) component of the IR beam. The PEM is orientated in such a way that the incident light is polarized in a plane which is at 45° to its main axis. After reflection on the surface, the IR beam is focused onto the mercury cadmium telluride (MCT) detector by an optical lens. After demodulation, two spectra are obtained corresponding to $(p + s)$ and $(p - s)$ signals. By combining these spectra, the gas phase insensitive to polarization changes, and the adsorbate phase which is orientated by the surface and else very sensitive to polarization changes can be separated. Only the p-component of the IR beam will contribute to the surface signal, while both p and s components participate in the gas phase signal. The surface signal is obtained from the ratio of these spectra, $(p - s)/(p + s)$, while the gas phase signal is obtained from the s signal. Spectra collected during the reaction are then normalized by the corresponding reference spectra. The spectra were collected with a spectral resolution of 4 cm^{-1}, with 1024 scans co-added. The PEM was operated in the half-wave retardation mode, at a frequency of 50 kHz.

The Pt(111) and $Pt_3Sn(111)$ samples are small discs of 1.0 and 0.8 cm diameter, respectively. They were prepared by repeated cycles of Ar sputtering at 300 K and annealing at 1100 K for Pt(111) and 1000 K (600 K) for $Pt_3Sn(111)$-$p(2 \times 2)$ ($Pt_3Sn(111) - (\sqrt{3} \times \sqrt{3})$) respectively until a clean surface was observed by XPS. From time to time, the samples were oxidized in a few 10^{-6} Torr O_2 at 900 K to remove the carbonaceous contamination. Once cleaned, the sample is transferred under UHV to the reactor then heated to the temperature at which the reaction will take place. The reactor is then isolated by closing all the valves and reference spectra are measured at this temperature. The reactants are then introduced into the reactor and the reaction products are monitored by PM-RAIRS, QMS and gas phase chromatography. The reactor is operated in static mode. The reactive C_4H_6/H_2 mixture was prepared in a separate UHV chamber and stored into a large volume stainless steel vessel.

3. Results

In order to establish a close correlation between pure platinum and platinum–tin alloy properties, the following experiments have been run within the same conditions: temperature of the sample 360 K, partial pressure of C_4H_6 and H_2 in the ratio 1/10, total pressure in the reactor close to 15 Torr. The time between each experimental point is rather long due

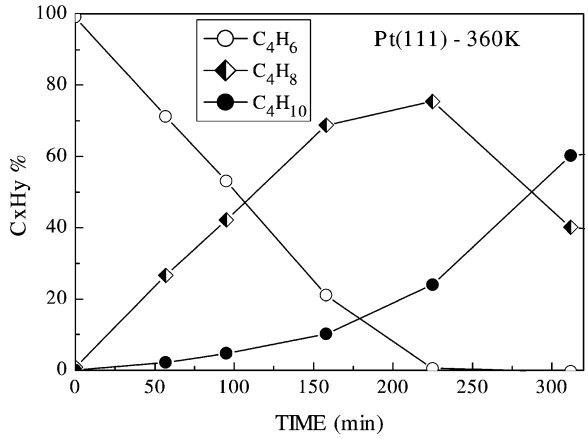

Fig. 1. Evolution of products measured by QMS during hydrogenation of 1,3-butadiene on Pt(111). Reaction conditions: $T = 360$ K, $p(H_2)/p(1,3\text{-butadiene}) = 10$, total pressure in the reactor = 15 Torr.

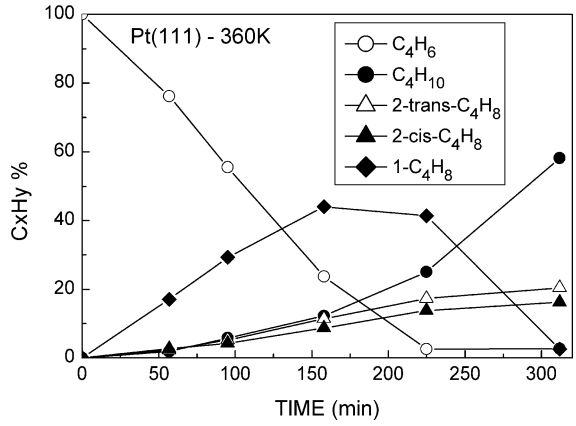

Fig. 2. Evolution of products measured by gas phase chromatography during hydrogenation of 1,3-butadiene on Pt(111). Reaction conditions: $T = 360$ K, $p(H_2)/p(1,3\text{-butadiene}) = 10$, total pressure in the reactor = 15 Torr.

to the successive measurements by the three different techniques, PM-RAIRS, QMS and gas phase chromatography.

3.1. Pt(111)

Fig. 1 shows the evolution of the reactants and products 1,3-butadiene, butenes (1-butene + *cis*-2-butene + *trans*-2-butene not separated by QMS), and butane measured by mass spectroscopy as a function of time. Only the first part of the reaction is shown corresponding to the total conversion of 1,3-butadiene. In fact, the reaction has been tested until complete conversion which was obtained after 1200 min. At low conversion and up to 50% conversion, the selectivity into butenes S_1 defined as: $S_1 = \sum\text{butenes}/\sum(\text{butenes} + \text{butane})$ reaches a value close to 89% then decreases slightly until 80% conversion. The activity is equal to 4.7×10^{15} mol cm^{-2} s^{-1}. Compared to Pt(111) at 300 K [4,10], this reaction performed at 360 K is more active but also more selective.

More information is produced by gas phase chromatography, since the three butene isomers are now separated. The results are reported in Fig. 2. The 1-butene is the most abundant of the butene isomers until complete conversion. Then it starts to decrease while the cis and trans isomers increase continuously until complete conversion of butenes. The selectivity into 1-butene S_2 defined as $S_2 = \text{1-butene}/\sum\text{butenes}$ is 0.87 at 50% conversion. The *cis*/*trans* ratio is 0.86 at 50% conversion and decreases slightly to 0.72 at higher conversion.

Fig. 3 shows the evolution of the gas phase measured by IR as a function of reaction time at 360 K. At the very beginning of the reaction (Fig. 3a), the IR spectrum is similar to the gas phase spectrum of pure 1,3-butadiene with bands in the range of 2976–3108 cm^{-1} corresponding to a combination of symmetric and asymmetric νCH and νCH_2 stretching vibrations and at 1013 cm^{-1}, 987 cm^{-1} and 908.4 cm^{-1} characteristic of the CH bending, CH_2 rocking and CH_2 wagging deformation vibrations, respectively.

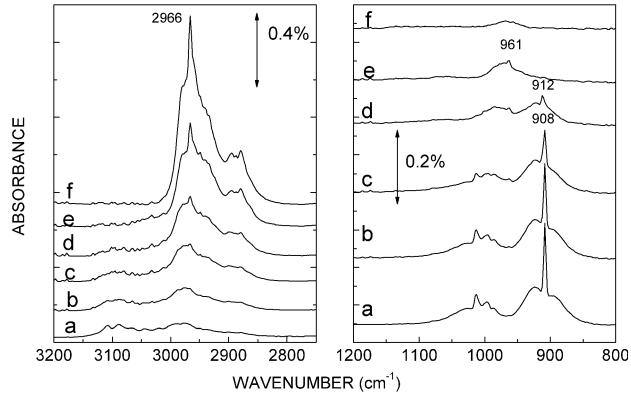

Fig. 3. Evolution of the reaction products measured by PM-RAIRS during 1,3-butadiene hydrogenation on Pt(111) at 360 K as a function of time: (a) 20 min, (b) 1 h, (c) 2 h, (d) 3 h, (e) 4.5 h and (f) 19.5 h. Reaction conditions: $T = 360$ K, $p(H_2)/p(1,3\text{-butadiene}) = 10$, total pressure in the reactor = 15 Torr.

With increasing reaction time, the features characteristic of 1,3-butadiene decrease while gradually new bands develop, namely at 2966 cm^{-1} (Fig. 3c–f), 912 cm^{-1} (Fig. 3d) and 961 cm^{-1} (Fig. 3f). In order to highlight the changes appearing in the gas phase, difference spectra obtained by rationing a current spectrum by the immediately preceding one are reported in Fig. 4. Positive bands indicate the presence of new species while negative bands indicate the consumption of a product. For comparison the gas phase spectra characteristic of pure 1,3-butadiene, butenes and butane are reported. 1,3-Butadiene, 1-butene and butane spectra have been measured in our system, while the spectra for *cis*- and *trans*-2-butene are issued from the literature [22]. The difference spectra, $\Delta(b-a)$, $\Delta(c-b)$, $\Delta(d-c)$, and $\Delta(e-d)$, correspond to equivalent reaction times, viz about 1 h. They can be compared with each other. The last one shows what happens during the last 15 h of the reaction. The first spectrum, $\Delta(b-a)$, clearly shows a decrease of the bands at around 3100 cm^{-1} and at 1018 and 908 cm^{-1} indicating the consumption of 1,3-butadiene. In the mean time, new

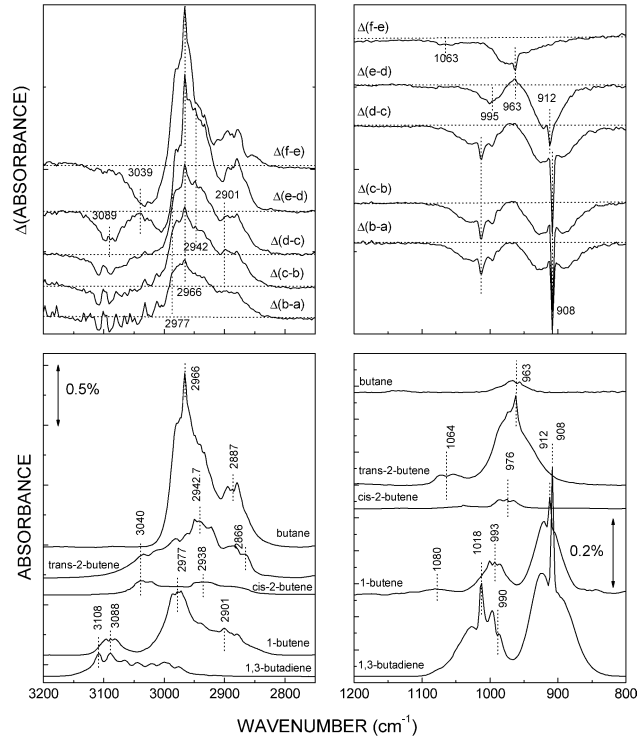

Fig. 4. Difference spectra between successive IR data of the previous figure. For comparison, the gas phase spectra obtained on pure butadiene, 1-butene, *cis*- and *trans*-2-butene, and butane are reported. Spectra corresponding to 1,3-butadiene, 1-butene and butane have been measured during this work while those for *cis*- and *trans*-2-butene are from literature [22]. Except for the *trans*-2-butene, where the measurement pressure was not indicated, all the gas phase spectra are normalized to a common pressure.

positive bands are observed at 2942 cm^{-1} and 2977 cm^{-1} indicating the formation of new products which, from the reference spectra, can be attributed to 1-butene and butane. From this spectrum, corresponding to a 1,3-butadiene conversion of less than 25%, we cannot exclude the presence of *cis*- and *trans*-2-butenes. As the reaction proceeds, the intensity of the most sensitive bands of butadiene remains constant (see curves $\Delta(c-b)$ and $\Delta(d-c)$) indicating a linear decrease of butadiene content as a function of time, in perfect agreement with the QMS and chromatography results. Meanwhile, the characteristic band of butane at 2942 cm^{-1} increases more rapidly than that of 1-butene at 2977 cm^{-1}. Later on, spectrum $\Delta(e-d)$ clearly shows a negative band at 3089 cm^{-1} indicating the consumption of 1-butene. This observation is corroborated by the decrease of the bands at 995 and 912 cm^{-1}. Finally, in the last 15 hours, as shown in spectrum $\Delta(f-e)$, the negative bands observed at 3039, 1063 and 963 cm^{-1} indicate the consumption of *trans*-2-butene at the benefit of butane formation.

3.2. $Pt_3Sn(111)$-$(\sqrt{3}\times\sqrt{3})$ and $Pt_3Sn(111)$-p(2 × 2)

The reactivity of $Pt_3Sn(111)$ has been studied under similar conditions for both surface structures ($\sqrt{3}\times\sqrt{3}$) and p(2 × 2).

Fig. 5 exhibits the mass spectroscopy results obtained at 160 K for the $Pt_3Sn(111)$-($\sqrt{3}\times\sqrt{3}$). Compared to Pt(111) (see Fig. 1), the activity is quite lower but the product distribution indicates a more selective conversion of 1,3-butadiene. During the 1,3-butadiene decrease, only a small amount of butane is formed: less than 1% at 50% conversion while it was close to 6% on Pt(111). The selectivity into butenes S_1 is 98% at 50% conversion and keeps this value until 90% of conversion. The activity is equal to 0.5×10^{15} mol cm^{-2} s^{-1}, i.e., ten times less than that of Pt(111). The gas phase chromatography spectra not reported here show that the selectivity into 1-butene S_2 is 79% at 50% conversion with a *cis*/*trans* ratio of 0.85.

The enhancement of selectivity with respect to Pt(111) is also illustrated in Fig. 6 by IR spectra of the gas phase. The spectra clearly show, as a function of time, the decrease of 1,3-butadiene bands, the formation of 1-butene (Fig. 6d–f) identified by the bands at 3088, 2976 and 984 cm^{-1}, followed by an increased production of *trans*-2-butene identified by the band at 963 cm^{-1}. As said previously, the observation of *cis*-2-butene is not straightforward since it does not possess a real fingerprint on the spectra due to a large band overlap.

On the $Pt_3Sn(111)$-p(2 × 2) surface, both activity and selectivity are still slightly improved by comparison to $Pt_3Sn(111)$-($\sqrt{3}\times\sqrt{3}$). The QMS and IR results are reported in Figs. 7 and 8. The activity is 0.6×10^{15} mol cm^{-2} s^{-1}. The selectivity into butenes S_1 is now more than 99% at 50% conversion. This high selectivity is confirmed by IR results in Fig. 8, where no butane which would lead to the appearance of a sharp band at 2966 cm^{-1} is observed until complete conversion of butadiene (Fig. 8f–g).

All these results show a very good complementarity between the three techniques used in this work. It would have been very interesting to observe also the surface species present during the reaction since the PM-RAIR spectroscopy is a good tool for doing so; however, no surface species has

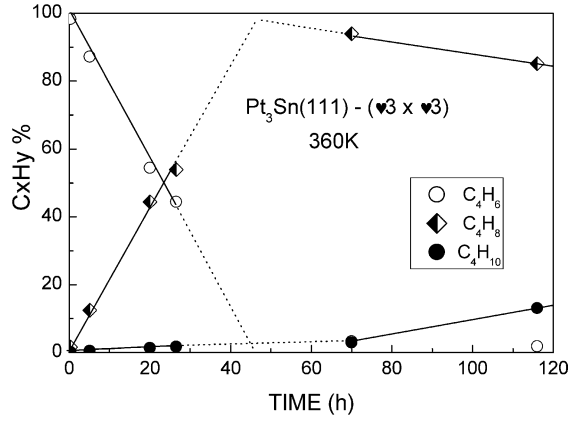

Fig. 5. Evolution of the products measured by QMS during hydrogenation of 1,3-butadiene on $Pt_3Sn(111)$-($\sqrt{3}\times\sqrt{3}$) at 360 K. $p(H_2)/p$(1,3-butadiene) = 10, total pressure in the reactor = 14.5 Torr.

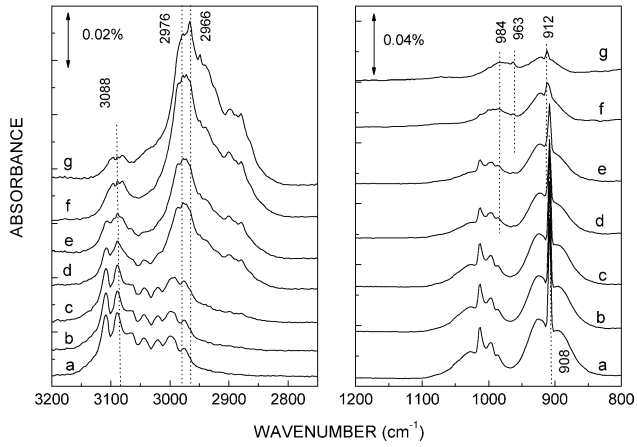

Fig. 6. Evolution of the reaction products measured by PM-RAIRS during 1,3-butadiene hydrogenation on $Pt_3Sn(111)$-$(\sqrt{3}\times\sqrt{3})$ as a function of time: (a) 15 min, (b) 1.35 h, (c) 5 h, (d) 19.5 h, (e) 28.2 h, (f) 69.45 h and (h) 116 h. Reaction conditions: $T = 360$ K, $p(H_2)/p(1,3\text{-butadiene}) = 10$, total pressure in the reactor = 14.5 Torr.

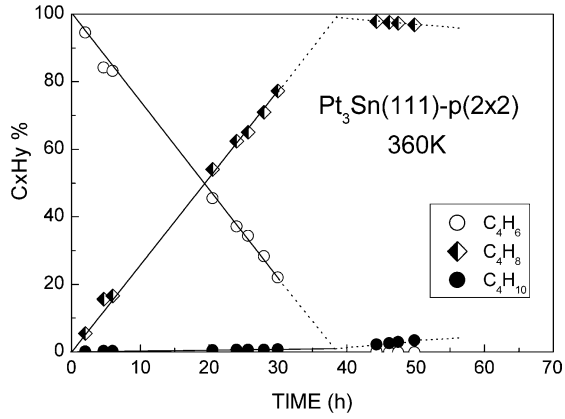

Fig. 7. Evolution of the products measured by QMS during hydrogenation of 1,3-butadiene on $Pt_3Sn(111)$-p(2 × 2) at 360 K. $p(H_2)/p(1,3\text{-butadiene}) = 10$, total pressure in the reactor = 14.2 Torr.

been observed. Several reasons can explain the nonobservation of surface species (adsorbate or intermediate). The adsorption geometry may be not propitious to measurements by RAIRS. Let us just remind that only the dipole moment variations having a component along the normal to the surface will contribute to the RAIRS signal. For example, in the case of a 1,3-butadiene molecule lying flat on the surface, no CH or CC stretching vibration band is observable by RAIRS. On the contrary, a signal is expected for the out of plane CH deformation bands. However, it also greatly depends on the IR activity of these bands. As observed in Fig. 4, when the stretching bands are intense, the corresponding deformation ones are small and vice versa. Concerning the nonobservation of intermediates species, it can be due to their very short lifetime on the surface, especially at the temperature of the reaction (360 K), but also to a very small amount of such species on the surface.

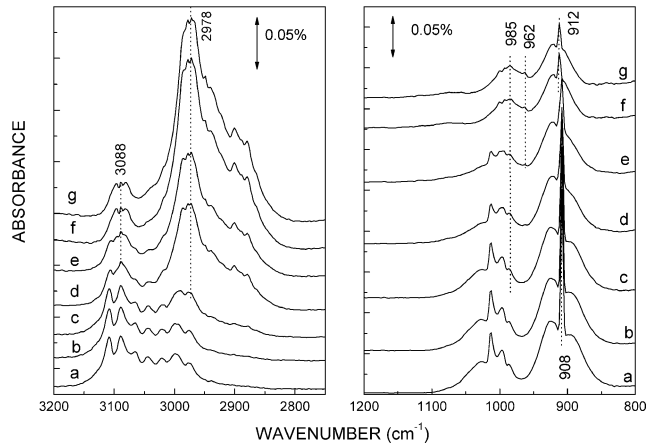

Fig. 8. Evolution of the reaction products measured by PM-RAIRS during 1,3-batadiene hydrogenation on $Pt_3Sn(111)$-p(2 × 2) as a function of time: (a) 15 min, (b) 1.20 h, (c) 5.15 h, (d) 19.30 h, (e) 25.0 h and (f) 43.40 h and (h) 53.30 h. Reaction conditions: $T = 360$ K, $p(H_2)/p(1,3\text{-butadiene}) = 10$, total pressure in the reactor = 14.2 Torr.

4. Discussion

1,3-butadiene hydrogenation on the three studied surfaces, Pt(111), $Pt_3Sn(111)$-$(\sqrt{3}\times\sqrt{3})$ and $Pt_3Sn(111)$-p(2 × 2), is characterized by a linear decrease of the 1,3-butadiene content with time (see Figs. 1, 5 and 7) indicating a constant reaction rate. This suggests that the reaction does not depend on the 1,3-butadiene pressure and that it is of a zero order with respect to the hydrocarbon.

Whatever the surface, Pt(111) or $Pt_3Sn(111)$, the catalytic activity remains constant up to about 80% conversion. Similarly the butane, *cis*- and *trans*-2-butenes relative amounts increase linearly with time in the same range of percentage conversion.

The values of the activity and of the percentages of butane and butenes determined at 50% conversion are reported in Table 1. On Pt(111), the selectivity into butenes S_1 (89%) is actually more than that measured near 300 K on Pt(111) [10], Pt films [23], and Pt/Al_2O_3 supported catalysts [19,24]. Let us just remark that in the present work, the reaction was run at 360 K while most measurements reported in the literature were performed near 300 K and with a smaller hydrogen/1,3-butadiene ratio which could explain the apparent discrepancy. Thus, for example, Pradier et al. [4] have seen noticeable variations of the adsorption of the different products with temperature on Pt single crystals. The *trans*/*cis* ratio of 2-butene is slightly larger than unity, a value which differs again from that measured on nonselective Pt films [23] and Pt/Al_2O_3 supported catalysts for which it is about two [19,24].

The activity of both the $(\sqrt{3}\times\sqrt{3})$ and the p(2 × 2) surfaces of the $Pt_3Sn(111)$ alloy is one order of magnitude lower than that of Pt(111) but the selectivity into butenes is largely increased by comparison to pure platinum; this effect is even more pronounced on the $Pt_3Sn(111)$-p(2 × 2) surface structure for which the butane content is only 0.5%.

Table 1
Activity, butane % and butene composition measured on Pt(111), $Pt_3Sn(111)$-$(\sqrt{3}\times\sqrt{3})$ and $Pt_3Sn(111)$-p(2×2) at 50% conversion, 360 K and a total pressure of 15 Torr (p_{H_2}/p(1,3-butadiene) = 10)

Sample	Activity	Butane	Composition (%)		
	(10^{15} mol cm^{-2} s^{-1})	(%)	1-Butene	*cis*-2-Butene	*trans*-2-Butene
Pt(111)	4.7	11	74	12	14
$Pt_3Sn(111)$-$(\sqrt{3}\times\sqrt{3})$	0.5	2	79	10	11
$Pt_3Sn(111)$-p(2×2)	0.6	0.5	–	–	–

As observed with Pt(111), the 1-butene is the most abundant product on the alloy surfaces and the relative amount of 2-butene isomers is almost the same.

It has been often proposed that the distribution of the products may depend on the adsorption state of 1,3-butadiene [23] and on its adsorption strength relative to that of adsorbed butenes. Recent theoretical calculations [18] on Pt(111) suggest that the 1,2,3,4-tetra-σ adsorption state, in which all the carbon atoms interact with Pt, is the most probable (adsorption energy = -160 kJ mol^{-1}) at low coverage followed by the 1,4-di-σ-2,3-π and 1,2-di-σ-3,4-π states slightly less strongly adsorbed. The observation of a zero order with respect to 1,3-butadiene in this experiment is indicative of a surface saturated in reactive hydrocarbonated species, i.e., in which the hydrocarbon coverage is high. In such a case, the repulsive interactions between ad-molecules would lead to different adsorption states. A more slightly di-σ bonded species appear then as the most probable [18]. In that case, the adsorbed state of butenes resemble those of 1,3-butadiene with a very similar adsorption energy, calculated at -45 kJ mol^{-1}. The desorption of butenes (via its competition with butadiene) is thus not favored and rather leads to a catalyst poorly selective into butenes.

In the case of the Pt_3Sn-$(\sqrt{3}\times\sqrt{3})$ and $Pt_3Sn(111)$-p(2×2) ordered structures, the presence of the tin atoms may play two major roles in connection with their catalytic properties. Firstly, due to the geometric arrangement of surface atoms (Fig. 9) some adsorption states of the butadiene molecules which were available on Pt(111) are not allowed anymore if one assumes that the tin surface atoms are inactive. For example, the 1,2,3,4-tetra-σ adsorption state, considered as the most favorable at low hydrocarbon coverage on pure platinum, is not possible on the alloy since it would require a specific diamond-shaped site made of 4 Pt atoms. Secondly, and probably more important, is the dilution effect played by the surface tin atoms. In fact, even if the surface is saturated into 1,3-butadiene, these Sn atoms which are ordered on the surface will contribute to move away the 1,3-butadiene molecules from each other (less available sites) and then to lower the interactions between ad-molecules. One can then think of possible adsorption of 1,3-butadiene through di-$\sigma+\pi$-bonding. Such ad-molecules would be less reactive but would avoid the formation of butane by increasing the competition in favor of adsorbed butadiene (di-$\sigma+\pi$-bonded) with respect to adsorbed butenes (di-σ-bonded). It would have been very important to identify the reactive species at surface, but unfortunately, as said previously, PM-

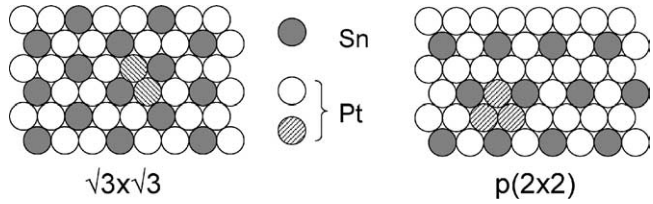

Fig. 9. Scheme of the $Pt_3Sn(111)$ surface structures following [20]. Shaded circles are shown here to highlight the Pt sites (binary with the $(\sqrt{3}\times\sqrt{3})$ and ternary with the p(2×2) surfaces respectively.

RAIRS measurements have not allowed the observation of such species.

Other effects could also be invoked to explain the differences between pure Pt and Pt_3Sn alloy: the presence on the studied surfaces of different intermediates species, which probably are in too low concentration and of too short lifetime to be simply observed, and electronic interactions between platinum atoms and the neighbouring tin atoms. By use of CO as a probe molecule on Pt and PtSn catalysts, it has been shown that tin induces only a small shift ($+6$ cm^{-1}) of the νCO stretching vibration interpreted as a decrease of the electron density of platinum atoms when alloyed to tin [25]. In this work, due to the lack of resolution of a standard XPS analyser, it was not possible to show on the Pt4f core levels any chemical shift between Pt(111) and $Pt_3Sn(111)$. In fact, Rodríguez et al. [26] from ab initio SCF calculations have shown that the Pt–Sn bond is complex, involving a Sn(5s,5p) → Pt(6s,6p) charge transfer and a Pt5d → Pt(6s,6p) rehybridization that localizes electrons in-between the metal centers. More recently, Janin et al. [27] have shown by high resolution photoelectron spectroscopy performed on $Pt4f_{7/2}$ core levels of Pt(111), Pt(111)–Sn(2×2) and Pt(111)–Sn$(\sqrt{3}\times\sqrt{3})$ a negative surface core level shift of -370, -210 and -230 meV respectively relative to the bulk value. The shift induced by tin on Pt is thus small, in the range of 140–160 meV and certainly not measurable by standard XPS.

5. Summary and conclusions

The present work shows that the 1,3-butadiene reacts selectively on $Pt_3Sn(111)$ and more precisely when the surface is p(2×2) reconstructed. This increase of selectivity is accompanied by a decrease of activity. The role of tin can be tentatively explained by dilution effects leading to specific

adsorption sites with reduced molecular interactions and probably new adsorption states of different adsorption energies. A comparative study of chemisorption of 1,3-butadiene and butenes on Pt(111) and Pt_3Sn(111) surfaces is now important to strengthen these conclusions. Anyhow, these first results show that PtSn could be a catalyst of interest for selective hydrogenation of 1,3-butadiene.

Acknowledgments

The authors acknowledge U. Bardi and collaborators from the University of Florence for supplying their Pt_3Sn(111) crystal and P. Ruiz for his help in running chromatography experiments.

References

[1] J.P. Boitiaux, J. Cosyns, E. Robert, Appl. Catal. 35 (1987) 193.
[2] J. Goetz, D.Y. Murzin, M.L. Ulischenko, R. Touroude, Chem. Eng. Sci. 51 (1996) 2879.
[3] A. Molnar, A. Sarkani, M. Varga, J. Mol. Catal. A: Chem. 173 (2001) 185.
[4] C.M. Pradier, E. Margot, Y. Berthier, J. Oudar, Appl. Catal. 43 (1988) 177.
[5] J.C. Bertolini, Y. Jugnet, in: D.P. Woodruff (Ed.), Surface Alloys and Alloy Surfaces, Elsevier, Amsterdam, 2002, p. 404.
[6] H. Ogasawara, S. Ichihara, H. Okuyama, K. Domen, M. Kawai, J. Electron. Spectrosc. Relat. Phenom. 114–116 (2001) 339.
[7] S. Katano, S. Ichihara, H. Ogasawara, H.S. Kato, T. Komeda, M. Kawai, K. Domen, Surf. Sci. 502–503 (2002) 164.
[8] J.C. Bertolini, A. Cassuto, Y. Jugnet, J. Massardier, B. Tardy, G. Tourillon, Surf. Sci. 349 (1996) 88.
[9] J. Massardier, J.C. Bertolini, A. Renouprez, in: M.J. Philips, M. Teman (Eds.), Proceedings of the 9th International Congress on Catalysis, 1988, p. 1222.
[10] J. Massardier, J.C. Bertolini, J. Catal. 90 (1984) 358.
[11] Y. Gauthier, R. Baudoing, Y. Joly, J. Rundgren, J.C. Bertolini, J. Massardier, Surf. Sci. 162 (1985) 342.
[12] F. Coloma, J. Llorca, N. Homs, P. Ramírez de la Piscina, F. Rodríguez-Reinoso, A. Sepúlveda-Escribano, Phys. Chem. Chem. Phys. 2 (2000) 3063.
[13] G.F. Santori, M.L. Casella, G.J. Siri, H.R. Adúriz, O.A. Ferretti, Appl. Catal. A 197 (2000) 141.
[14] G.F. Santori, A.G. Moglioni, V. Vetere, G.Y. Moltrasio Iglesias, M.L. Casella, O.A. Ferretti, Appl. Catal. A 269 (2004) 215.
[15] S.M. Stagg, C.A. Querini, W.E. Alvarez, D.E. Resaco, J. Catal. 168 (1997) 75.
[16] J. Llorca, N. Homs, J. León, J. Sales, J.L.G. Fierro, P. Ramírez de la Piscina, Appl. Catal. A 189 (1999) 77.
[17] T. Gjervan, R. Prestvik, A. Holmen, in: Basic Principles in Chemical Physics, in: Springer Series in Chemical Physics, 2004, p. 127.
[18] A. Valcarcel, A. Clotet, J.M. Ricart, F. Delbecq, P. Sautet, Surf. Sci. 549 (2004) 121.
[19] D.A.G. Aranda, M. Schmal, J. Catal. 171 (1997) 398.
[20] S. Speller, U. Bardi, in: D.P. Woodruff (Ed.), Surface Alloys and Alloy Surfaces, Elsevier, Amsterdam, 2002, p. 184.
[21] L.J. Shorthouse, Y. Jugnet, J.C. Bertolini, Catalysis Today 70 (2001) 33.
[22] *cis*- and *trans*-2-butene spectra are issued from the NIST Webbook, http://webbook.nist.gov.
[23] R.B. Moyes, P.B. Welles, J. Grant, N.Y. Salman, Appl. Catal. A 229 (2002) 251.
[24] E.M. Crabb, R. Marshall, Appl. Catal. A 217 (2001) 41.
[25] E. Merlen, P. Beccat, J.C. Bertolini, P. Delichère, N. Zanier, B. Didillon, J. Catal. 159 (1996) 178.
[26] J.A. Rodríguez, S. Chaturvedi, T. Jirsak, J. Hrbek, J. Chem. Phys. 109 (1998) 4052.
[27] E. Janin, H. von Schenck, S. Ringler, J. Weissenrieder, T. Åkermark, M. Göthelid, J. Catal. 215 (2003) 245.